ELSEVIER

Journal of Alloys and Compounds 336 (2002) 5–10

Journal of ALLOYS AND COMPOUNDS

www.elsevier.com/locate/jallcom

Mössbauer and DSC studies of spin reorientations in $Er_{2-x}Y_xFe_{14}B$

A.T. Pedziwiatr*, B.F. Bogacz, R. Gargula, S. Wróbel

Institute of Physics, Jagiellonian University, Reymonta 4, 30-059 Cracow, Poland

Received 26 July 2001; accepted 7 August 2001

Abstract

Polycrystalline $Er_{2-x}Y_xFe_{14}B$ (x=0.0, 0.5, 1.0, 1.5) compounds have been studied by ^{57}Fe Mössbauer spectroscopy and differential scanning calorimetry (DSC) in the temperature range 80–370 K. The spin reorientation phenomenon has been studied extensively by narrow step temperature scanning in the vicinity of the spin reorientation temperature. Using the procedure of subtracting the Mössbauer spectra taken for the same compound at different temperatures, it was possible to follow the influence of transition on the shape of spectra. From this procedure it was concluded that in the region of transition, each subspectrum splits into two Zeeman sextets, which are characterised by different hyperfine fields and quadrupole splittings. A consistent way of describing the Mössbauer spectra was proposed. The composition and temperature dependencies of hyperfine interaction parameters and subspectra contributions were derived from experimental spectra. Endothermic DSC peaks were observed for all compounds studied which correspond to the transition from basal plane to axial easy magnetisation direction. The spin reorientation temperatures and the enthalpies of transitions were established from the DSC data. A spin arrangement diagram was constructed and spin reorientation temperatures obtained by different methods were compared. © 2002 Elsevier Science B.V. All rights reserved.

Keywords: Transition metal compounds; Rare earth compounds; Anisotropy; Mössbauer spectroscopy; Thermal analysis

1. Introduction

The Er-based $R_2Fe_{14}B$ (R=rare earth) systems exhibit many interesting magnetic properties including spin reorientation phenomena. $Er_2Fe_{14}B$ changes its spin arrangement at the spin reorientation temperature, T_{SR}, of 316 K [1]. Up till now, several groups [2–12] have studied the nature of spin reorientation phenomena in yttrium substituted $Er_{2-x}Y_xFe_{14}B$ compounds trying to establish the role of the Er sublattice anisotropy.

In these compounds the magnetocrystalline anisotropy changes from planar to axial (along the *c*-axis) with increasing temperature. The actual easy magnetisation direction of $Er_{2-x}Y_xFe_{14}B$ depends on the temperature-induced competition between the uniaxial Fe sublattice anisotropy [13] and the basal plane Er sublattice anisotropy [14].

The $Er_{2-x}Y_xFe_{14}B$ intermetallic compounds crystallise in a tetragonal structure with space group $P4_2/mnm$ [15]. The iron atoms occupy six non-equivalent crystal sites ($16k_1$, $16k_2$, $8j_1$, $8j_2$, 4*e*, 4*c*). The rare earth ions occupy the 4*f* and 4*g* crystallographic sites and boron is located at the 4*g* site.

In this study, the polycrystalline $Er_{2-x}Y_xFe_{14}B$ (x=0.0, 0.5, 1.0, 1.5) compounds have been investigated by ^{57}Fe Mössbauer spectroscopy using narrow step temperature scanning and by differential scanning calorimetry (DSC) in order to establish the spin reorientation temperatures, to determine the temperature region of spin reorientation and the influence of reorientation on hyperfine parameters. Our goal was also to propose a consistent description of the Mössbauer spectra in the whole range of temperatures and to study the thermal effects connected with this magnetic transition.

2. Experimental

The $Er_{2-x}Y_xFe_{14}B$ (x=0.0, 0.5, 1.0, 1.5) compounds were produced by a standard procedure of induction melting under flowing high purity argon and subsequent annealing at 900°C for 2 weeks. X-Ray and thermomagnetic analysis proved the single phase state of the materials, however, the Mössbauer spectra indicated a small amount of natural iron impurity in $Er_2Fe_{14}B$ (about 2%) and in $ErYFe_{14}B$ (about 1%). These small impurity

*Corresponding author. Fax: +48-12-633-7086.

E-mail address: ufpedziw@if.uj.edu.pl (A.T. Pedziwiatr).

0925-8388/02/$ – see front matter © 2002 Elsevier Science B.V. All rights reserved.
PII: S0925-8388(01)01872-2

patterns were subtracted from the experimental spectra by a numerical procedure. The ^{57}Fe Mössbauer transmission spectra were recorded in the temperature range 80–340 K. The spin reorientation phenomenon near T_{SR} has been studied extensively by narrow step (sometimes 1 K) temperature scanning using a ^{57}Co(Rh) source and a computer-driven constant acceleration mode spectrometer. A high purity iron foil was used to calibrate the velocity scale. Isomer shifts were established with respect to the centre of gravity of the room temperature iron Mössbauer spectrum. Samples of $Er_{2-x}Y_xFe_{14}B$ (x=0.0, 0.5, 1.0, 1.5) have also been studied by DS-calorimetry in the temperature range 170–370 K. The measurements were carried out in heating and cooling cycles at rates ranging from 5 to 30 K/min.

3. Data analysis

Selected experimental Mössbauer spectra of the $Er_{1.5}Y_{0.5}Fe_{14}B$ intermetallic compound are shown in Fig. 1. The 'exponential' approximation [16] of the transmission integral was used to describe the investigated Mössbauer spectra, as in Ref. [12]. A simultaneous constrained fitting of several Mössbauer spectra gave us the opportunity to establish consistently the temperature dependence of the hyperfine parameters. The spectra below and above the temperature region of spin reorientation were analysed using six Zeeman subspectra with relative intensities according to iron occupation of the crystallographic sublattices (4:4:2:2:1:1). Each subspectrum was characterised by the following hyperfine parameters: magnetic field, *H*, isomer shift, *IS*, quadrupole splitting, *QS* (defined as $[(V_6-V_5)-(V_2-V_1)]/2$ where V_i are velocities corresponding to Mössbauer line positions).

Due to systematic difficulties in describing the experimental Mössbauer spectra in the transition region, we used a procedure, which allowed us to observe direct changes in the shape of Mössbauer spectra: two spectra of the same compound recorded at different temperatures were numerically subtracted. The procedure of subtraction was preceded by the correction of the subtracted spectrum which took into consideration the temperature changes of *IS* and *H*. Values of the changes per 1 K $\left(\frac{\Delta IS}{\Delta T}, \frac{\Delta H}{\Delta T}\right)$ were determined on the basis of the analysis of the Mössbauer spectra recorded beyond the spin reorientation region. Fig. 2 shows some of the results for $Er_2Fe_{14}B$. The subtraction of spectra recorded at narrow step temperature intervals allowed us to observe relatively sudden changes connected with the spin reorientation. The result of the subtraction of spectra taken at different temperatures is shown in Fig. 2. In the first graph (320–321 K) these spectra subtract entirely giving only the base line. 'Differential spectra' obtained at higher temperatures (323–324, 324–325, 325–326 K) show visible changes occurring during the reorientation. In the presented 'differential spectra' the lines disappearing during the reorientation process (with the increase in temperature) are observed in the form of 'absorption' lines and the lines appearing after the spin reorientation are observed in the form of 'scattering' lines. The last graph in Fig. 2 (332–333 K) represents the end of the spin reorientation process: changes are no longer visible. The analysis presented above shows the temperature range of the reorientation process.

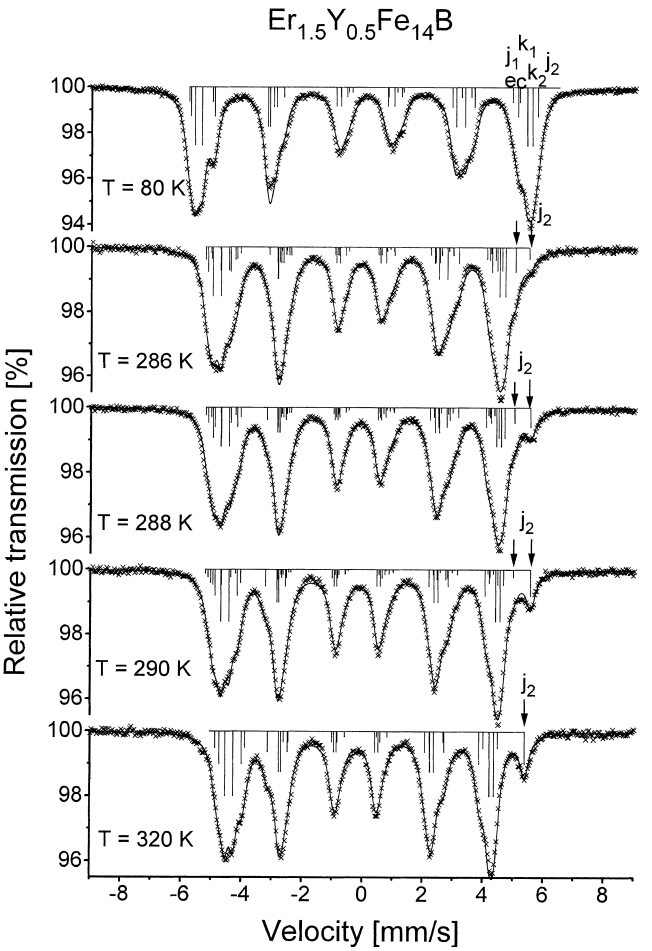

Fig. 1. Selected ^{57}Fe Mössbauer transmission spectra for the $Er_{2-x}Y_xFe_{14}B$ (x=0.5) intermetallic compound. The solid lines are fits to the data. The bar diagrams show the line positions and relative intensities. Positions of the sixth line of $8j_2$ sextets are specially marked. In the transition region $8j_2$ has two positions, corresponding to 'low' and 'high temperature' Zeeman sextets, marked by arrows.

Fig. 3 shows the subtraction of spectra recorded at 320 K (before the spin reorientation) and at 334 K (after the spin reorientation). One can clearly see the changes in spectra occurring in the spin reorientation process. A temperature correction of *IS* and *H* in the spectrum taken at higher temperature was introduced. The bar diagrams show the line positions and their relative intensities (in the 334 K spectrum after temperature correction). It was

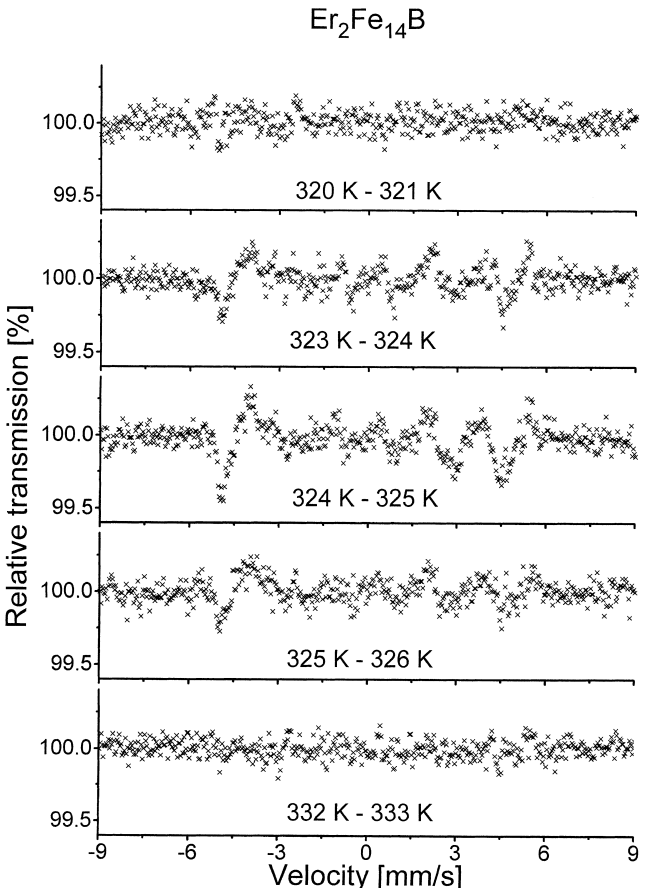

Fig. 2. Selected differential spectra for $Er_2Fe_{14}B$. The lines disappearing during the reorientation process (with increase in temperature) are observed in the form of 'absorption' lines and the lines appearing after spin reorientation are observed in the form of 'scattering' lines.

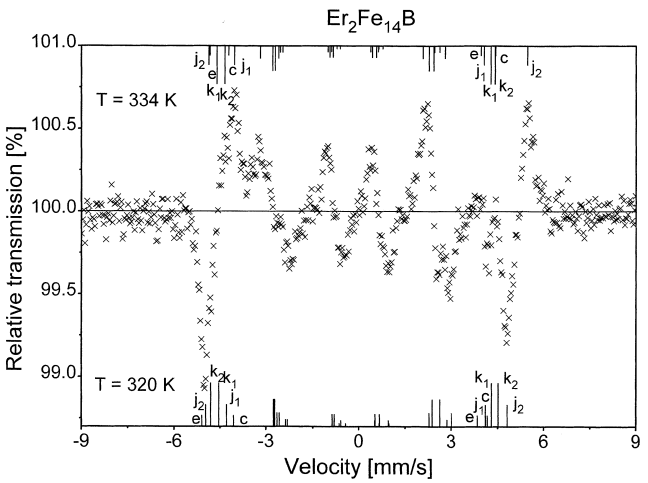

Fig. 3. Differential spectrum (320–334 K) for $Er_2Fe_{14}B$. A temperature correction of *IS* and *H* in the spectrum taken at 334 K was taken into account. The bar diagrams show the line positions and relative intensities (in the higher temperature after temperature correction).

observed that the changes in the right part of the spectrum concern mainly the position of the sixth line of the $8j_2$ sextet. In the left part of the spectrum, the first line of the $16k_2$ sextet changes its position. It is difficult to attribute other changes to one single concrete sublattice. Thus, we conclude that all sublattices take part in the spin reorientation collectively. This direct observation of changes in the experimental Mössbauer spectra during the spin reorientation allowed us to propose the following description: Mössbauer spectra below the spin reorientation region can be described by 'low temperature' Zeeman sextets and those above by 'high temperature' Zeeman sextets. There is a coexistence of the 'low' and 'high temperature' Zeeman sextets in the region of the transition. Both kinds of Zeeman sextets exchange gradually (between themselves) their contributions C_l, C_h to the total spectrum and have different values of *H* and *QS*. Weak, systematic changes of *H* and *QS* with temperature were taken into account for spectra below and above the spin reorientation region. A common linear temperature dependence of IS caused by the second-order Doppler shift effect was assumed for the 'low' and 'high temperature' Zeeman

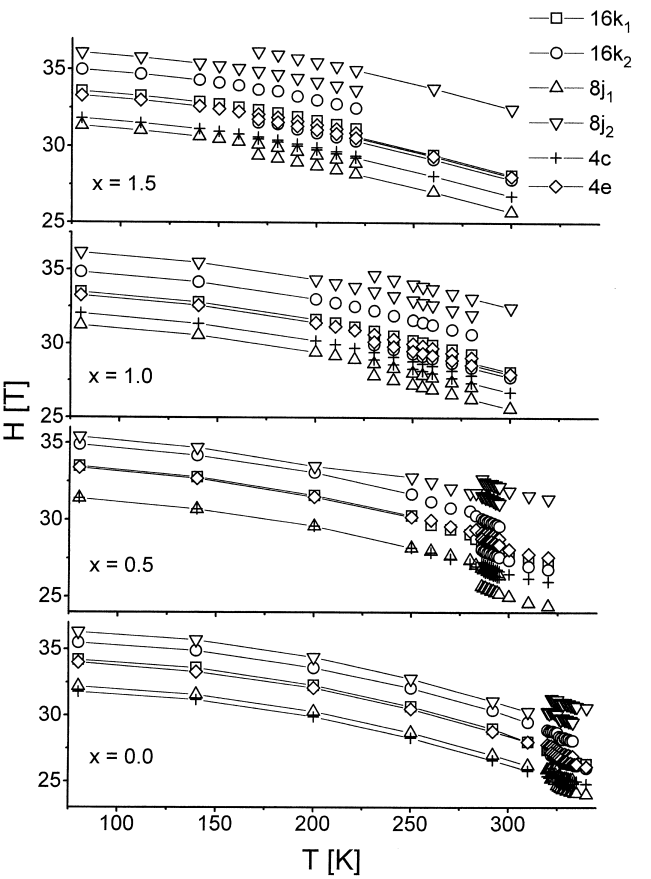

Fig. 4. Temperature dependencies of the hyperfine field *H* for different crystal sites of the $Er_{2-x}Y_xFe_{14}B$ ($x = 0.0$ [12], 0.5, 1.0, 1.5). The average error is 0.1 T. The dual assignment in the spin reorientation region is connected with the co-existence of 'low' and 'high temperature' sextets.

sextets. This description is similar to the procedure applied for polycrystalline $Er_2Fe_{14}B$ [12].

One of our goals was to find the temperature range of the spin reorientation phenomenon and to determine the spin reorientation temperature using Mössbauer spectroscopy. The most useful feature which enables us to do this is the separation of the sixth line in the $8j_2$ subspectrum of the analysed experimental spectra. Owing to the clear development of its intensity in the course of the transition, it was possible to establish precisely the contribution of the 'high temperature' Zeeman part of the $8j_2$ sublattice to the spectrum and to determine the spin reorientation temperature.

4. Results and discussion

The temperature dependencies of the hyperfine fields derived from the spectra for the $Er_{2-x}Y_xFe_{14}B$ system are shown in Fig. 4. The assignment of H to the crystal sublattices was based on the nearest neighbour argument [17]. The hyperfine field decreases with the increase in temperature below and above the region of the spin reorientation for all sublattices. In the region of transition we observed experimentally that each Zeeman sextet splits into two parts.

The behaviour of QS is connected with the change of angle between the easy axis of magnetisation and the electric field gradient [18]. The QS parameters are almost independent of temperature below and above the region of transition (Fig. 5). For the $8j_2$ sublattice, some changes of the QS parameter in the initial part of the reorientation region were observed for all $Er_{2-x}Y_xFe_{14}B$ compounds studied. The behaviour of H and QS in $Er_{2-x}Y_xFe_{14}B$ ($x=0.5$, 1.0, 1.5) is similar to that observed in $Er_2Fe_{14}B$ [12].

Subspectra contributions C_l, C_h of both 'low' and 'high temperature' Zeeman sextets, correspondingly, are shown in Fig. 6. From this plot, we derived the spin reorientation temperature (assumed to be at the intersection point of the C_l and C_h curves) for $Er_{2-x}Y_xFe_{14}B$ ($x=0.0$ [12], 0.5, 1.0, 1.5). It was observed that the substitution of Y for Er causes a decrease in T_{SR} and an increase in the temperature range of the spin reorientation. The values of the spin reorientation temperature determined from Mössbauer

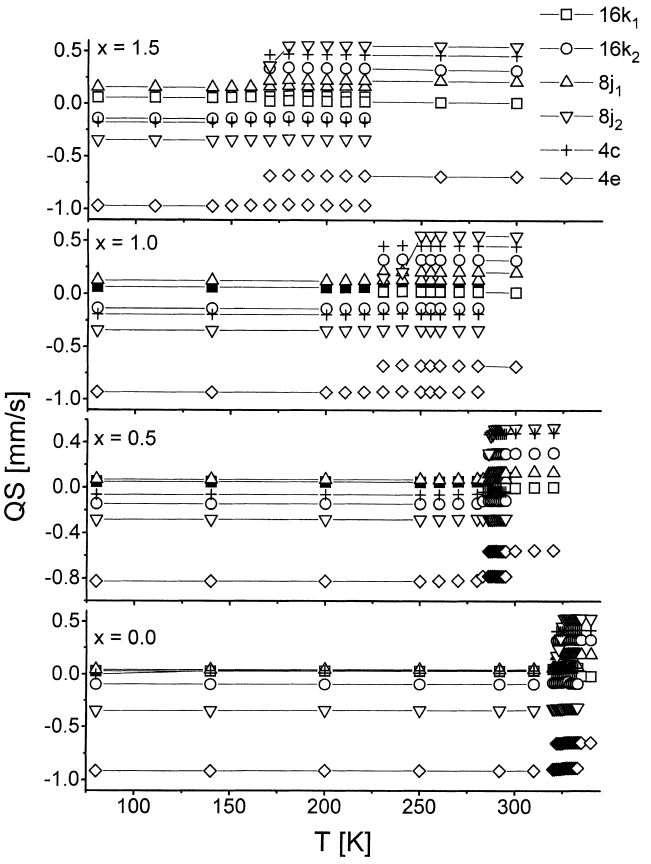

Fig. 5. Temperature dependencies of the quadrupole splitting QS for different crystal sites of the $Er_{2-x}Y_xFe_{14}B$ ($x=0.0$ [12], 0.5, 1.0, 1.5). The average error is 0.01 mm/s. The dual assignment in the spin reorientation region is connected with the co-existence of 'low' and 'high temperature' sextets.

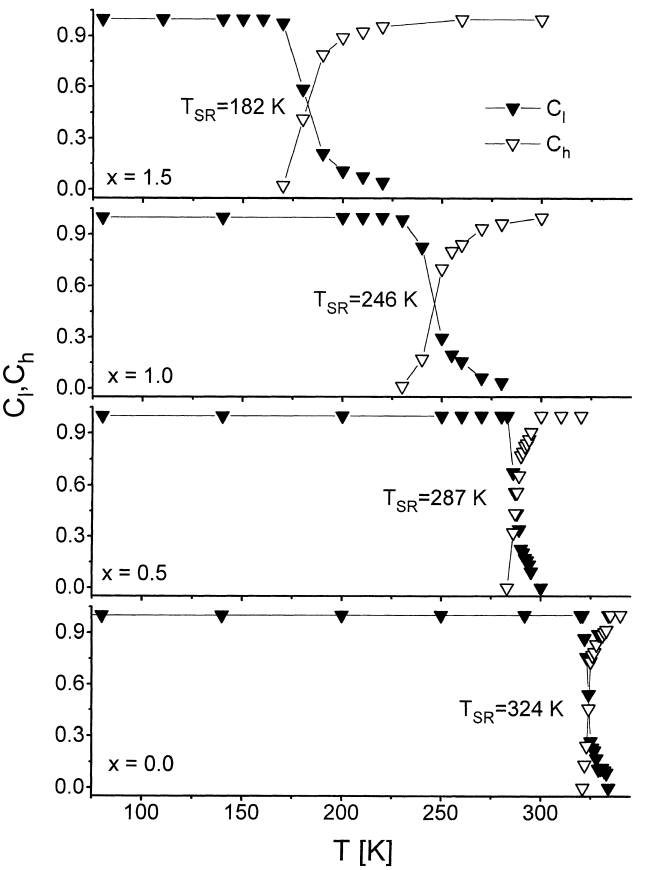

Fig. 6. Temperature dependencies of subspectra contributions for both C_l —'low temperature' (solid triangle) and C_h — 'high temperature' (open triangle) Zeeman sextets. The average error is 0.1.

Table 1
Values for the spin reorientation temperature

Compound	T_{SRM} (K)	T_{SRC} (K)	ΔH (J/g)
$Er_2Fe_{14}B$	324±1	326±1	0.32±0.04
$Er_{1.5}Y_{0.5}Fe_{14}B$	287±1	288±1	0.30±0.04
$ErYFe_{14}B$	246±2	242±2	0.29±0.06
$Er_{0.5}Y_{1.5}Fe_{14}B$	182±2	179±2	0.25±0.07

T_{SRM}, by Mössbauer effect; T_{SRC}, by DSC and values of enthalpy of the transition; ΔH, for $Er_{2-x}Y_xFe_{14}B$ ($x=0.0$ [12], 0.5, 1.0, 1.5).

measurements, T_{SRM}, for all compositions studied are given in Table 1.

Fig. 7 illustrates the DS-calorimetry observation of thermal effects in the $Er_{2-x}Y_xFe_{14}B$ systems in the vicinity of the spin reorientation. Endothermic peaks correspond to the transition of the easy magnetisation direction from the basal plane to the *c*-axes for all compounds studied. The spin reorientation temperatures were established as arithmetic average temperatures of heating (index *h*) and cooling (index *c*) peak positions $\left(T_{SR}=\frac{T_{SRh}+T_{SRc}}{2}\right)$. The values of the spin reorientation temperatures determined from DSC measurements T_{SRC} for all compounds studied are given in Table 1. The enthalpy ΔH of the transition (corresponding to the area under the DSC peaks) was calculated as the arithmetic average of the absolute values obtained from the heating and cooling cycles. The values of ΔH for $Er_{2-x}Y_xFe_{14}B$ are given in Table 1.

The spin phase diagram for the $Er_{2-x}Y_xFe_{14}B$ systems is shown in Fig. 8. It compares the results of spin reorientation temperatures obtained by different methods (Mössbauer effect, DSC and magnetic measurements [6]), showing a good agreement. By diluting the Er sublattice with nonmagnetic yttrium, the range of axial anisotropy becomes larger and the T_{SR} value decreases.

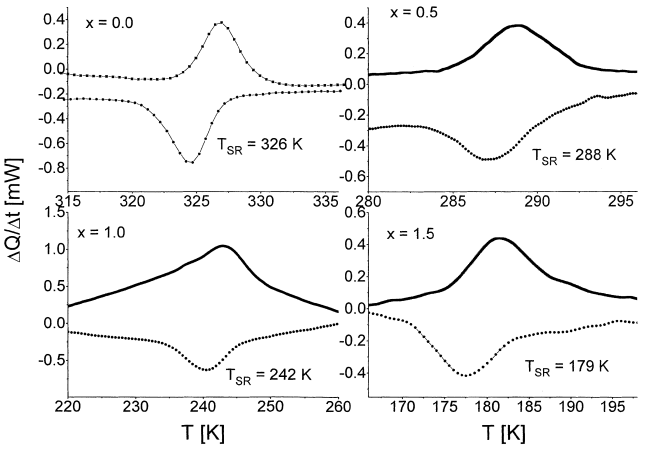

Fig. 7. Endothermic transition due to the spin reorientation measured by differential scanning calorimetry for the $Er_{2-x}Y_xFe_{14}B$ ($x=0.0$, 0.5, 1.0, 1.5) compounds. Upper and lower curves show the results of measurements, which were performed on heating (*h*-indices) and cooling (*c*-indices), respectively, both at a rate of 30 K/min.

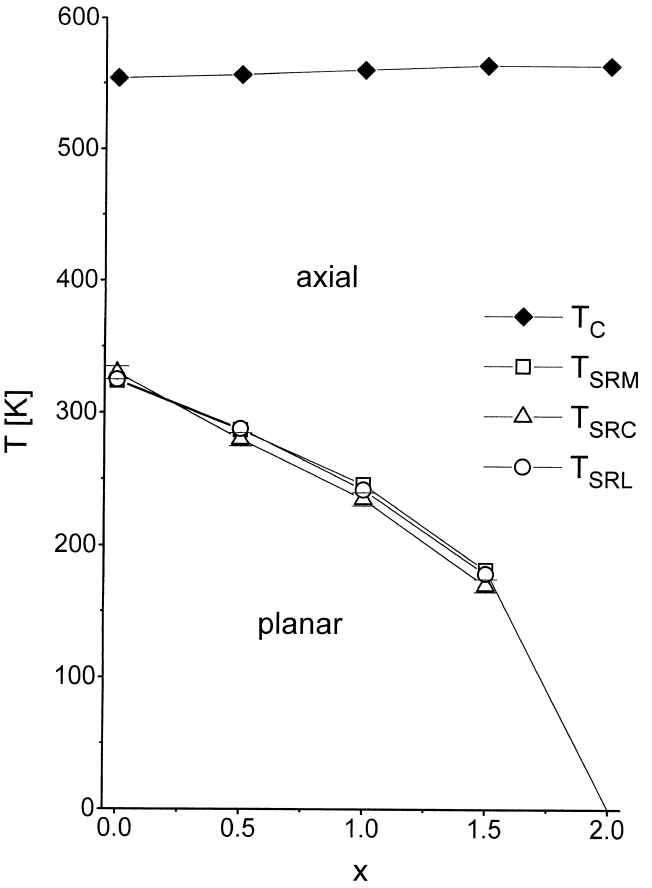

Fig. 8. Spin structure phase diagram for the $Er_{2-x}Y_xFe_{14}B$ system. T_C, Curie temperature [6]; T_{SRM}, spin reorientation temperature determined from Mössbauer measurements; T_{SRC}, spin reorientation temperature determined from DSC data; T_{SRL}, spin reorientation temperature determined from magnetic measurements [6].

References

[1] S. Hirosawa, M. Sagawa, Solid State Commun. 54 (1985) 335.
[2] A. Vasquez, J.M. Friedt, J.P. Sanchez, Ph. L'Héritier, R. Fruchart, Solid State Commun. 55 (1985) 783.
[3] K.H.J. Buschow, in: E.P. Wohlfarth, K.H.J. Buschow (Eds.), Ferromagnetic Materials, Vol. 4, Elsevier, Amsterdam, 1988.
[4] K.H.J. Buschow, Rep. Prog. Phys. 54 (1991) 1123.
[5] E. Burzo, Rep. Prog. Phys. 61 (1998) 1099.
[6] A.T. Pedziwiatr, W.E. Wallace, J. Less-Common Met. 126 (1986) 41.
[7] M. Abe, S.H. Liou, C.L. Chien, N.C. Koon, B.N. Das, E. Callen, J. Appl. Phys. 61 (8) (1987) 3568.
[8] C.D. Fuerst, J.F. Herbst, E.A. Alson, J. Magn. Magn. Mater. 54–57 (1986) 567.
[9] N.C. Koon, B.N. Das, C.M. Williams, J. Magn. Magn. Mater. 54–57 (1986) 523.
[10] C. Piqué, R. Burriel, L.M. García, F.J. Lázaro, J. Bartolomé, J. Magn. Magn. Mater. 104 (1992) 1167.
[11] J.S. Garitaonandia, J.M. Barandiarán, I. Orue, F. Plazaola, M.R. Ibbarra, A. del Moral, J. Magn. Magn. Mater. 140 (1995) 949.
[12] R. Wielgosz, A.T. Pedziwiatr, B.F. Bogacz, S. Wróbel, Mol. Phys. Rep. 30 (2000) 167.
[13] D. Givord, H.S. Li, R. Perrier de la Bâthie, Solid State Commun. 51 (1984) 857.

[14] S. Hirosawa, Y. Matsuura, H. Yamamoto, S. Fujimura, M. Sagawa, H. Yamauchi, J. Appl. Phys. 59 (1986) 873.
[15] J.F. Herbst, J.J. Croat, F.E. Pinkerton, W.B. Yelon, Phys. Rev. B29 (1984) 4176.
[16] B.F. Bogacz, Mol. Phys. Rep. 30 (2000) 15.
[17] G.J. Long, F. Grandjean, Supermagnets — Hard Magnetic Materials, NATO ASI Series, Kluwer, Dordrecht, 1990, p. 261.
[18] P. Gütlich, R. Link, A. Trautwein, Mössbauer Spectroscopy and Transition Metal Chemistry, Springer, Berlin, 1978.